Reciprocal hemizygosity analysis reveals that the *Saccharomyces cerevisiae CGI121* gene affects lag time duration in synthetic grape must

Runze Li and Rebecca C. Deed ![ORCID] *

School of Chemical Sciences and School of Biological Sciences, University of Auckland, Auckland 1142, New Zealand

*Corresponding author: School of Chemical Sciences and School of Biological Sciences, University of Auckland, 3A Symonds Street, Auckland 1010, New Zealand. rebecca.deed@auckland.ac.nz

Abstract

It is standard practice to ferment white wines at low temperatures (10–18°C). However, low temperatures increase fermentation duration and risk of problem ferments, leading to significant costs. The lag duration at fermentation initiation is heavily impacted by temperature; therefore, identification of *Saccharomyces cerevisiae* genes influencing fermentation kinetics is of interest for winemaking. We selected 28 *S. cerevisiae* BY4743 single deletants, from a prior list of open reading frames (ORFs) mapped to quantitative trait loci (QTLs) on Chr. VII and XIII, influencing the duration of fermentative lag time. Five BY4743 deletants, Δ*apt1*, Δ*cgi121*, Δ*clb6*, Δ*rps17a*, and Δ*vma21*, differed significantly in their fermentative lag duration compared to BY4743 in synthetic grape must (SGM) at 15°C, over 72 h. Fermentation at 12.5°C for 528 h confirmed the longer lag times of BY4743 Δ*cgi121*, Δ*rps17a*, and Δ*vma21*. These three candidates ORFs were deleted in *S. cerevisiae* RM11-1a and S288C to perform single reciprocal hemizygosity analysis (RHA). RHA hybrids and single deletants of RM11-1a and S288C were fermented at 12.5°C in SGM and lag time measurements confirmed that the S288C allele of *CGI121* on Chr. XIII, encoding a component of the EKC/KEOPS complex, increased fermentative lag phase duration. Nucleotide sequences of RM11-1a and S288C *CGI121* alleles differed by only one synonymous nucleotide, suggesting that intron splicing, codon bias, or positional effects might be responsible for the impact on lag phase duration. This research demonstrates a new role of *CGI121* and highlights the applicability of QTL analysis for investigating complex phenotypic traits in yeast.

Keywords: fermentation; lag time; quantitative trait loci; reciprocal hemizygosity analysis; wine; yeast

Introduction

Alcoholic fermentation for most white wines is performed at low temperatures (10–18°C), as this range generally results in greater production and retention of desirable volatiles, leading to high-quality wines (Llauradó *et al.* 2002; Molina *et al.* 2007; García-Ríos *et al.* 2017). However, low temperatures also dramatically lengthen the time taken until fermentation completion and increase the risk of ferments becoming stuck or sluggish, which is potentially costly in terms of reduced winery space, product loss, and decreased profits (Bisson 1999; Colombie *et al.* 2005; Llauradó *et al.* 2005; Beltran *et al.* 2007; López-Malo *et al.* 2013). Low temperatures encountered during fermentation are particularly stressful to yeast and cause changes in cell membrane fluidity, nutrient uptake and utilization, production of protective compounds, and a decrease in enzymatic reaction rates (Beltran *et al.* 2007; Redón *et al.* 2011; García-Ríos *et al.* 2016; Ganucci *et al.* 2018). A greater understanding of the genetics behind the ability of the wine yeast, *Saccharomyces cerevisiae*, to acclimate to low temperatures and perform fermentation more efficiently in general, is therefore useful for the wine industry.

The duration of the lag period at the start of fermentation, defined as the time between inoculation and the start of CO_2 release, and representing the time necessary for a yeast strain to acclimate to a new environment (Marullo *et al.* 2006), is greatly impacted by fermentation temperature, along with other variables encountered by yeast during fermentation. The high osmolarity of grape musts, along with the low pH, low-oxygen availability, oxidative stress, and potentially high levels of sulfur dioxide (SO_2), low levels of nutrients such as nitrogen, and to a lesser and strain-specific extent, phytosterols and thiamine, all contribute to the duration of the fermentative lag (Treu *et al.* 2014; Ferreira *et al.* 2017). Different *S. cerevisiae* strains also exhibit large variation in their fermentative lag duration ranging from a few hours up to a few days (Marullo *et al.* 2006; Camarasa *et al.* 2011). The genetic regulation controlling phenotypic variation in the fermentative lag time of different yeast strains is as complex as the variables involved and largely polygenic (Marullo *et al.* 2006, 2007). During the first few hours after inoculation in enological conditions, yeast must respond to the new environment with a dramatic metabolic reorganization, resulting in an increase in

the synthesis of transcripts and proteins involved in carbon and nitrogen metabolism, cellular stress response, ribosomal biogenesis, protein synthesis and oxidative stress (Rossignol *et al.* 2003; Salvadó *et al.* 2008). Within this response, there are likely to be numerous genes and quantitative trait loci (QTLs) that influence the duration of the lag phase before the release of CO_2. This response is more pronounced when the temperature of the must is low, lengthening the duration of the lag further (Salvadó *et al.* 2008; Albertin *et al.* 2017).

So far, one QTL with strong linkage to lag phase has been mapped to the *SSU1* gene, encoding the SO_2 efflux pump (Peltier *et al.* 2018). Removal of SO_2 from the yeast cell is carried out via Ssu1p, in which there are several allelic variants and translocation events in different strains that alter Ssu1p efficiency (Perez-Ortin *et al.* 2002; Ferreira *et al.* 2017). Beneficial genetic variants allow yeast to pump out SO_2 more efficiently, significantly reducing lag time. Previous work in our laboratory investigated QTLs linked to fermentation kinetics and found two regions, one of Chr. VII and one on Chr. XIII, that were significantly linked to fermentative lag (Deed *et al.* 2017). Linkage analysis was performed on a set of 119/121 completely mapped (>99% of the genome) F_1 progeny from a cross between haploid strains BY4716 and RM11-1a constructed by Brem *et al.* (2002). Due to the difficulty in phenotyping lag phase in experiments with grape juice, and the large number of candidate genes within the confidence intervals surrounding the high logarithm of the odds (LOD) score peaks on Chr. VII [10 open reading frames (ORFs)] and Chr. VIII (34 ORFs), these 44 candidate genes were not investigated further. This previous identification of chromosomal regions linked to lag phase duration provides an excellent opportunity to investigate the causative genes using a controlled and reproducible fermentation medium, such as synthetic grape must (SGM). Because single

reciprocal hemizygosity analysis (RHA) was not feasible for 44 different genes, we first aimed to test the lag duration of BY4743 single deletants of each candidate ORF identified in Deed *et al.* (2017). Those demonstrating variation in lag time compared to the BY4743 reference strain were deleted in haploids RM11-1a and S288C, followed by the construction of RHA hybrids. Phenotyping of deletants and RHA hybrids confirmed any relationships between the candidate ORFs with lag time phenotypes during fermentation.

Materials and methods
Saccharomyces cerevisiae strains
We utilized laboratory strain BY4743 (*MATa/α his3Δ1/his3Δ1 leu2Δ0/leu2Δ0 LYS2/lys2Δ0 met15Δ0/MET15 ura3Δ0/ura3Δ0*) and 28 BY4743 homozygous diploid deletants derived from EUROSCARF containing a Kanamycin resistance construct (*KanMX*) in place of each ORF of interest (Table 1). The deletants were selected based on an original list of 44 candidates linked to lag phase in Deed *et al.* (2017) after linkage analysis of 119/121 BY4716 × RM11-1a F_1 progeny using 2957 mapped loci (Brem *et al.* 2002). Of the 44 original candidates, 28 were available from EUROSCARF. Single gene deletions in three of the 28 candidates of interest were constructed in S288C (*MATα*), standing in for the BY4716 parent, and RM11-1a (*MATa HO::HphMX*) (Table 2). Combinations of wild-type and deletant versions of S288C and RM11-1a were then used to make hybrids for RHA.

Growth and fermentation conditions
S. cerevisiae cultures were propagated using yeast peptone dextrose (YPD) medium and incubated overnight at 28°C, with orbital shaking at 150 revolutions per minute (rpm). Pre-cultures were

Table 1 List of 28 ORFs identified within one LOD unit either side of the LOD >3 peak markers influencing lag phase duration in the *S. cerevisiae* genome and available as single deletions in BY4743 from EUROSCARF

Chromosome	LOD score	ORF	Gene	Function
VII	2.235–2.570	YGR104C	SRB5	Subunit of the RNA polymerase II mediator complex
VII	2.642–3.000	YGR105W	VMA21	Integral membrane protein required for V-ATPase function
VII	2.642–3.000	YGR106C	VOA1	ER protein that functions in assembly of the V0 sector of V-ATPase
VII	2.642–3.000	YGR107W	NA	Dubious open reading frame
VII	2.642–3.000	YGR108W	CLB1	B-type cyclin involved in cell cycle progression
VII	2.978	YGR109C	CLB6	B-type cyclin involved in DNA replication during S phase
VII	2.979–2.030	YGR110W	CLD1	Mitochondrial cardiolipin-specific phospholipase
XIII	2.606	YML048W	GSF2	Endoplasmic reticulum localized integral membrane protein
XIII	2.606–3.175	YML047C	PRM6	Potassium transporter that mediates K^+ influx
XIII	2.606–3.175	YML042W	CAT2	Carnitine acetyl-CoA transferase
XIII	2.606–3.175	YML041W	VPS71	Nucleosome-binding component of the SWR1 complex
XIII	3.175	YML038C	YMD8	Putative nucleotide sugar transporter
XIII	3.119–2.720	YML037C	NA	Putative protein of unknown function
XIII	2.478	YML036W	CGI121	Component of the EKC/KEOPS complex
XIII	2.547–3.681	YML035C	AMD1	AMP deaminase
XIII	2.547–3.681	YML034W	SRC1	Inner nuclear membrane protein
XIII	2.547–3.681	YML032C	RAD52	Protein that stimulates strand exchange
XIII	3.725–3.373	YML030W	RCF1	Cytochrome c oxidase subunit
XIII	3.725–3.373	YML029W	USA1	Scaffold subunit of the Hrd1p ubiquitin ligase
XIII	3.725–3.373	YML028W	TSA1	Thioredoxin peroxidase
XIII	3.725–3.373	YML027W	YOX1	Homeobox transcriptional repressor; binds to Mcm1p and early cell cycle boxes in promoters of cell cycle genes
XIII	3.725–3.373	YML026C	RPS18B	Protein component of the small (40S) ribosomal subunit
XIII	3.725–3.373	YML024W	RPS17A	Ribosomal protein 51 (rp51) of the small (40s) subunit
XIII	3.328	YML022W	APT1	Adenine phosphoribosyltransferase
XIII	3.421–3.288	YML021C	UNG1	Uracil-DNA glycosylase
XIII	3.421–3.288	YML020W	NA	Protein of unknown function
XIII	3.421–3.288	YML019W	OST6	Subunit of the oligosaccharyltransferase complex of the ER lumen
XIII	3.288	YML018C	NA	Protein of unknown function

Descriptions of protein function were obtained from the *Saccharomyces* Genome Database.

Table 2 List of RM11-1a and S288C RHA crosses to investigate the impact of the *CGI121*, *RPS17a*, and *VMA21* loci

Cross	Parent #1	Parent #2	F_1 hybrid selection
RM11-1a × S288C	RM11-1a (HO::HphMX; MATa)	**S288C (MATα)**	*HGM^R
RM11-1a × S288C Δcgi121	RM11-1a (HO::HphMX; MATa)	S288C (CGI121::KanMX; MATα)	HGM^R; Kan^R
RM11-1a × S288C Δrps17a	RM11-1a (HO::HphMX; MATa)	S288C (RPS17a::KanMX; MATα)	HGM^R; Kan^R
RM11-1a × S288C Δvma21	RM11-1a (HO::HphMX; MATa)	S288C (VMA21::KanMX; MATα)	HGM^R; Kan^R
RM11-1a Δcgi121 × S288C	RM11-1a (HO::HphMX; CGI121:: KanMX; MATa)	**S288C (MATα)**	*HGM^R; Kan^R
RM11-1a Δrps17a × S288C	RM11-1a (HO::HphMX; RPS17a:: KanMX; MATa)	**S288C (MATα)**	*HGM^R; Kan^R
RM11-1a Δvma21 × S288C	RM11-1a (HO::HphMX; VMA21:: KanMX; MATa)	**S288C (MATα)**	*HGM^R; Kan^R

The genotypes are given for each of the RM11-1a and S288C parents. The S288C parent strain in bold was required to be present in $100 \times$ excess of the RM11-1a parent, due to the lack of selectable markers to differentiate it from RM11-1a. The F_1 hybrid selections marked with * could result in the presence of the RM11-1a parent and the F_1 hybrid. The RM11-1a × S288c cross was included as a control.

Table 3 Oligonucleotide primers used for gene deletions and RHA

Primer name	Sequence (5′ to 3′)	Purpose
3'kanI-F	GGTCGCTATACTGCTGTC	Confirm integration of *KanMX* constructs
CGI121intL-F	CGGAATTAGCCCACGTAGAA	Amplification of *KanMX* from BY4743 Δcgi121 deletant
CGI121intR-R	GGAGAACTTTTGGCAGTTCG	Amplification of *KanMX* from BY4743 Δcgi121 deletant
CGI121testR-R	TATCGCAATGTCACCCCTTT	Flanking test primer to confirm integration of *KanMX* in the *CGI121* locus of transformants
RPS17aintL-F	GGCAGTGGTAGCTTGGTAGC	Amplification of *KanMX* from BY4743 Δrps17a deletant
RPS17aintR-R	CAGATGGCGTTTCATTTTG	Amplification of *KanMX* from BY4743 Δrps17a deletant
RPS17atestR-R	GGAGGAAACTGATTGGGTCA	Flanking test primer to confirm integration of *KanMX* in the *RPS17a* locus of transformants
VMA21intL-F	AGGAACCCTCCGCTTGTTAT	Amplification of *KanMX* from BY4743 Δvma21 deletant
VMA21intR-R	GGTTGGGCTTTTGAAGATGA	Amplification of *KanMX* from BY4743 Δvma21 deletant
VMA21testR-R	TTCCAAAACTGTGCAAGCAG	Flanking test primer to confirm integration of *KanMX* in the *VMA21* locus of transformants

washed in sterile water before further use via centrifugation for 5 minutes at $3,000\,g$. Growth curves were obtained using the Bioscreen C^{TM} MBR Automated Growth Curve Analysis System, operated via the BioScreener^{TM} software (Oy Growth Curves Ab Ltd.). Pre-cultures were used to inoculate YPD at 1×10^6 cells ml^{-1} in quintuplicate wells of a 100-well honeycomb plate. Cells were grown at 25°C for 72 h following the protocol in Deed et al. (2019). BY4743 and BY4743 deletion mutants were fermented in 250-ml flasks with airlock at 12.5°C and 15°C in 100 ml SGM modeled on the chemical composition of Sauvignon blanc grape juice (Henschke and Jiranek 1993; Kinzurik et al. 2015). For fermentations using the BY4743 strains, SGM was supplemented with additional amounts of the following amino acids: $10 \times$ histidine (300 mg L^{-1}), $10 \times$ leucine (300 mg L^{-1}), and $10 \times$ uracil (100 mg L^{-1}) (Harsch et al. 2010). RM11-1a and S288C wild types, deletants, and RHA hybrids were fermented at 12.5°C in 13-ml tubes with 8 ml SGM. A < 0.5 mm^2 pin-hole was punctured into each tube lid to allow for CO$_2$ escape (Deed et al. 2017). All fermentations were inoculated at density of 1×10^6 cells ml^{-1} and were monitored either 8-hourly or daily by measuring cumulative weight loss (g) (Bely et al. 1990).

Analysis of kinetic parameters

The length of fermentative lag phase (h) of BY4743 and the 28 BY4743 deletants at 15°C was determined using the cumulative weight loss data to calculate the time elapsed between inoculation and the x-axis intercept where the steepest part of the slope transects y_0, as per Marullo et al. (2006). Lag phase duration for all fermentations performed at 12.5°C was measured using a Gompertz model with curve fitting based on

Tronchoni et al. (2009) and executed using the R package nlstools (Baty et al. 2015).

Gene deletions and reciprocal hemizygosity analysis

Deletion of three candidate genes, *CGI121*, *RPS17a*, and *VMA21*, within either the Chr. VII or XIII QTLs linked to lag phase were constructed in RM11-1a Hgm^R and S288C using a modification of the Schiestl and Gietz (1989) lithium acetate yeast transformation protocol. Transformation of haploid RM11-1a and S288C was performed independently to generate mutants with *KanMX* insertions in *CGI121*, *RPS17a*, and *VMA21* by amplifying the corresponding constructs, *CGI121::KanMX*, *RPS17a::KanMX*, and *VMA21::KanMX*, from BY4743 EUROSCARF deletion library strains. Transformation with a Nat^R pFLR-A plasmid was used as a positive control. Successful deletions were confirmed via PCR (list of oligonucleotide primers in Table 3) and gel electrophoresis. Crosses were made between RM11-1a and S288C wild types, and combinations of nondeleted RM11-1a with each S288C deletion mutant and vice versa, in order to construct diploid hemizygous F_1 hybrids for RHA (Steinmetz et al. 2002b) (crosses in Table 2). Since there were no markers in the S288C parent, this strain had to be present in $100 \times$ excess of the RM11-1a deletion strain parent for mating (1×10^8 cells ml^{-1} S288C wild type with 1×10^6 cells ml^{-1} RM11-1a Hgm^R Kan^R deletion strain). Hybrids were selected on YPD plates containing 300 μg L^{-1} hygromycin B and 200 μg L^{-1} G-418. A multiplex PCR to amplify 10 variable microsatellite markers and two mating-type loci, *MATa* and *MATα*, was used to ensure that the hybridization was successful and to finalize strain selection since there would be some RM11-1a

Table 4 Microsatellite confirmation of F_1 hybrid strains between RM11-1a and S288C for RHA

Strain	C3	C5	C8	C4	091c	AT4	AT2	Scaat3	009c	267c	α	a
RM11-1a	121	139	146	259	260	296	364	381	419	—	—	480
S288C	120	174	130	240	303	296	358	407	443	—	457	—
RM11-1a x S288C	120, 121	139, 174	130, 146	240, 259	260, 303	296	358, 364	381, 407	419, 443	—	457	480
RM11-1a × S288C Δcgi121	120, 121	139, 174	130, 146	240, 259	260, 303	296	358, 364	381, 407	419, 443	—	457	480
RM11-1a × S288C Δrps17a	120, 121	139, 174	130, 146	240, 259	260, 303	296	358, 364	381, 407	419, 443	—	457	480
RM11-1a × S288C Δvma21	120, 121	139, 174	130, 146	240, 259	260, 303	296	358, 364	381, 407	419, 443	—	457	480
RM11-1a Δcgi121 × S288C	120, 121	139, 174	130, 146	240, 259	260, 303	296	358, 364	381, 407	419, 443	—	457	480
RM11-1a Δrps17a × S288C	120, 121	139, 174	130, 146	240, 259	260, 303	296	358, 364	381, 407	419, 443	—	457	480
RM11-1a Δvma21 × S288C	120, 121	139, 174	130, 146	240, 259	260, 303	296	358, 364	381, 407	419, 443	—	457	480

Numbers are band sizes in bp. The 12 loci detected correspond to 10 variable microsatellite loci and two mating-type loci, *MATa* and *MATα*, as described in Richards *et al.* (2009).

parents present when crossed with the marker-less S288C (Table 4) (Richards *et al.* 2009).

Statistical analysis and bioinformatics

All fermentation experiments were carried out in triplicate. Student's *t*-tests were carried out using Microsoft Excel with raw *p*-values reported, while ANOVA and *post hoc* Tukey's HSD were performed using JASP software (v. 0.12.2.0). Geneious Prime (v. 2020.2.1) was used to align nucleotide sequences and translate to amino acids and Clustal Omega (v. 1.2.4) was used to present the nucleotide alignments.

Data availability

The authors affirm that all data pertaining to this manuscript are either represented fully within the article and its tables and figures, along with the submission of Supplementary material on figshare: https://doi.org/10.25387/g3.14099213 (Supplementary File S1 containing the *CGI121* nucleotide sequence alignments for RM11-1a and S288C, Supplementary File S2 displaying the *BUD32*, *GON7*, *KAE1*, and *PCC1* alignments, and Supplementary Figure S1 showing growth curves for BY4743 and five BY4743 deletants in YPD at 25°C).

Supplementary material is available at https://doi.org/10.25387/g3.14099213.

Results

First screening of 28 BY4743 deletion mutants fermented in SGM at 15°C identified five candidate ORFs that may influence lag time

Of the 44 *S. cerevisiae* genes identified within the 95% confidence intervals of the high LOD score peaks for QTLs on Chr. VII and XIII linked to fermentation lag duration in Deed *et al.* (2017), 28 single-gene deletion mutants were available from EUROSCARF (listed in Table 1). Of the 16 ORFs that were unavailable, seven were classified as essential genes and hence inviable in a null mutant according to the Saccharomyces Genome Database. The remaining nine either encoded transposable elements (six ORFs) or were classified as dubious and unlikely to encode a protein (three ORFs). Cumulative weight loss (g) of the 28 BY4743 deletants fermented in 100 ml SGM at 15°C was measured at 8-h intervals for 72 h as a quick initial screen to identify whether any of the ORFs have an impact on the duration of the fermentative lag compared to the BY4743 reference (Figure 1, A–D). Because it

was not feasible to perform RHA on 28 different candidate genes, this initial step was conducted to narrow down the number of candidates. Due to the large number of fermentations in triplicate, the deletants were fermented in four separate batches, each with the BY4743 reference for standardization, and an uninoculated control as a measure of evaporation and to ensure there was no contamination.

Figure 1, A–D shows that the 28 deletants demonstrated a range of fermentation abilities at 15°C in SGM, with strong visual indications of variation in lag phase time compared to the BY4743 reference. The lag duration of BY4743 and the 28 deletants was calculated from the weight loss curves and presented in Figure 2, A–D. The lag time for BY4743 across the four batches ranged from 40 to 52.8 h, with a mean of 45.7 h ($n = 12$). This degree of variation demonstrates the difficulty of measuring lag time due to the high level of noise at the start of fermentation. There were no significant differences between the BY4743 deletants in batch 1 compared to BY4743 (Figure 2A). In batches 2 and 3, the lag phase times of BY4743 Δrps17a (56.6 h) (Figure 2B) and BY4743 Δvma21 (48.7 h) (Figure 2C) were significantly longer than BY4743 (43.6 h), while BY4743 Δclb6 (37.3 h) had a significantly shorter lag phase (Figure 2C). In batch 4, two deletants, BY4743 Δapt1 and BY4743 Δcgi121, had two replicates each that had not yet left lag phase (Figure 2D). For a useful comparison to be made against BY4743 (44.9 h), the lag times for these replicates were set at 70 h, giving an average duration of 63.5 h for BY4743 Δapt1 and 63.6 h for BY4743 Δcgi121, although the actual measure of lag time is likely to be longer for these deletants.

Further screening at 12.5°C confirms that BY4743 single deletions of Δcgi121, Δrps17a, and Δvma21 significantly alter fermentative lag time

Because the five candidate genes identified above were selected across three different fermentation batches with a degree of noise, and with some strains still in fermentative lag or unable to ferment, a repeat single-batch 100-ml fermentation was performed for the five deletants and BY4743 to confirm that the lag phase differences observed were repeatable. The fermentations were also performed over a longer timeframe (528 h) than was used previously to determine whether the mutants that did not initiate fermentation were still in lag phase or were unable to ferment. A temperature of 12.5°C was selected to provide a greater resolution in lag phase duration compared to 15°C, whilst maintaining an enologically relevant temperature. Prior to the
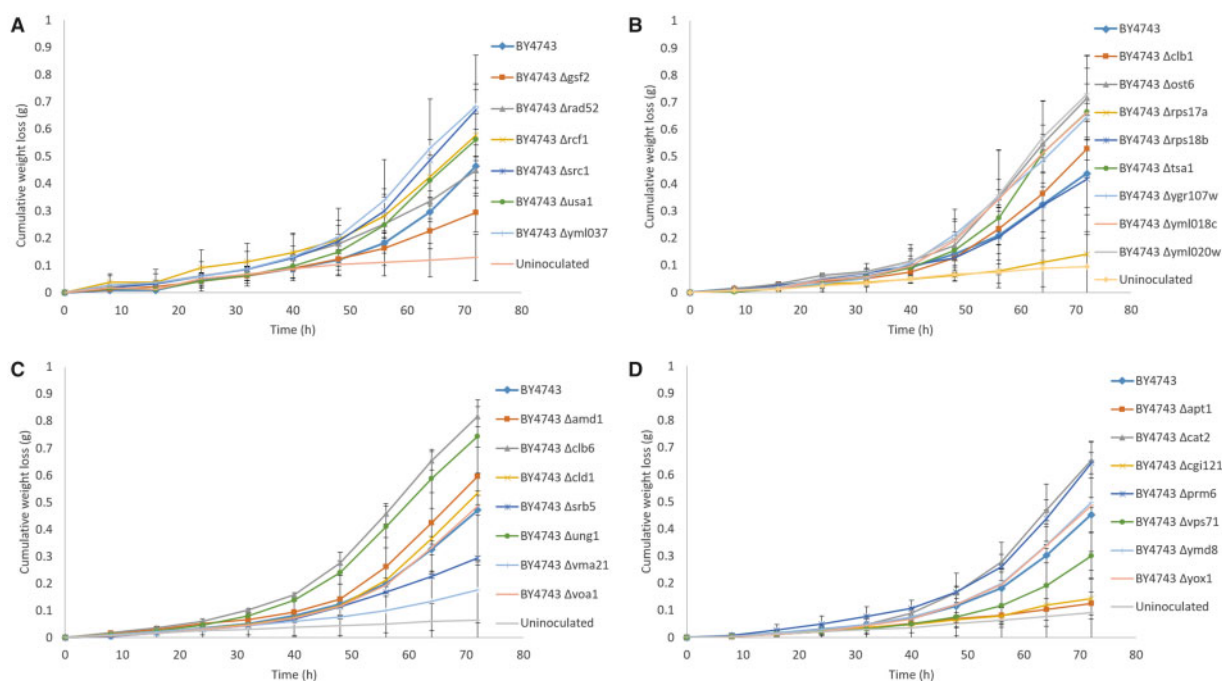
Figure 1 Average cumulative weight loss (g) of BY4743 and 28 BY4743 single gene deletion mutants fermented in SGM at 15°C for 72 h ($n = 3$). (A–D) Batches from 1 to 4 and each batch included BY4743 for standardization (series in bold). Error bars represent 95% confidence intervals.
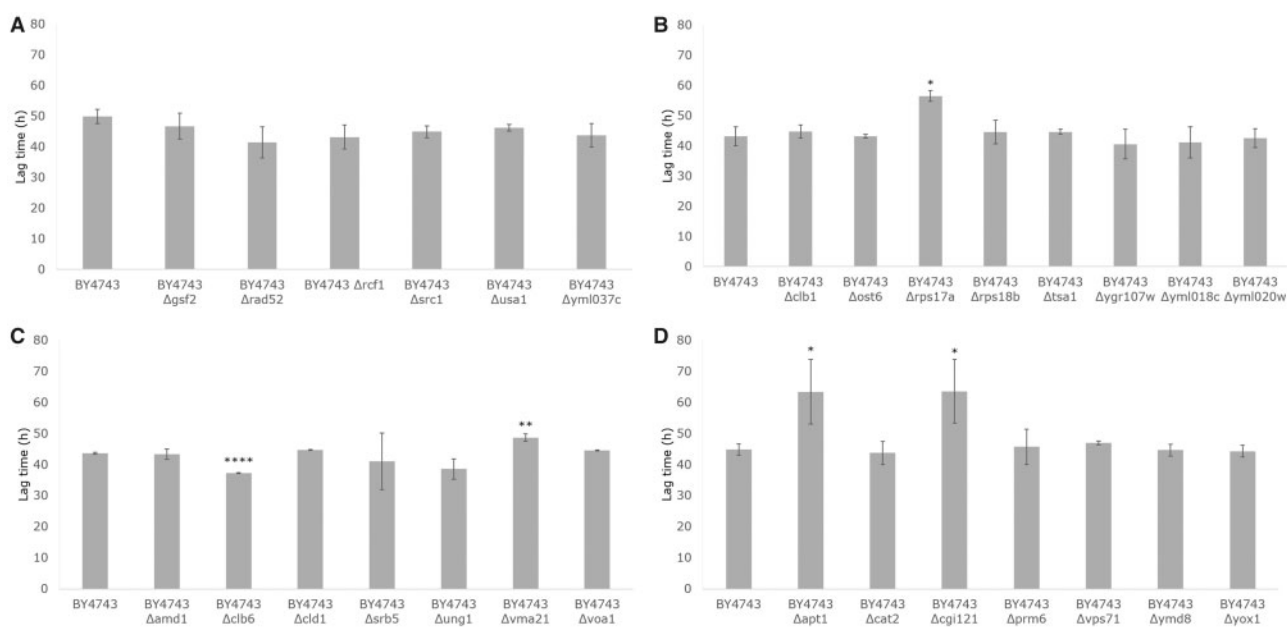

Figure 2 Lag time duration (h) of BY4743 and 28 BY4743 single-gene deletion mutants fermented in SGM at 15°C for 72 h ($n = 3$). (A–D) Batches from 1 to 4 and each batch included BY4743 for standardization. Error bars represent 95% confidence intervals. Student's t-test was used to generate P-values between BY4743 and every single deletant (*$P < 0.05$, **$P < 0.01$, ***$P < 0.001$, ****$P < 0.0001$).

fermentation experiment, the growth of the six strains in YPD at 25°C was also measured for 72 h to ensure that the number of viable cells in each YPD pre-culture was equivalent. This check was performed to ensure that potential variation in the starting number of live cells was not a factor, since differences would confound the length of fermentative lag. By ~24 h, all strains had reached stationary phase ensuring that the fresh inoculum added to each ferment, after adjusting based on cell counts, was the same (Supplementary Figure S1).

Figure 3 shows the weight loss curves at 12.5°C for the five deletants and BY4743. The results from the first screening at 15°C were conserved at 12.5°C, with BY4743 and BY4743 Δclb6 demonstrating an earlier exit from fermentative lag compared to BY4743 Δcgi121, BY4743 Δrps17a, and BY4743 Δvma21. Surprisingly, with the extension of the fermentation timeframe, it was revealed that the performance of the Δapt1 deletant was equivalent to the uninoculated control, with no initiation of fermentation. The Δapt1 deletant was capable of growth in YPD in
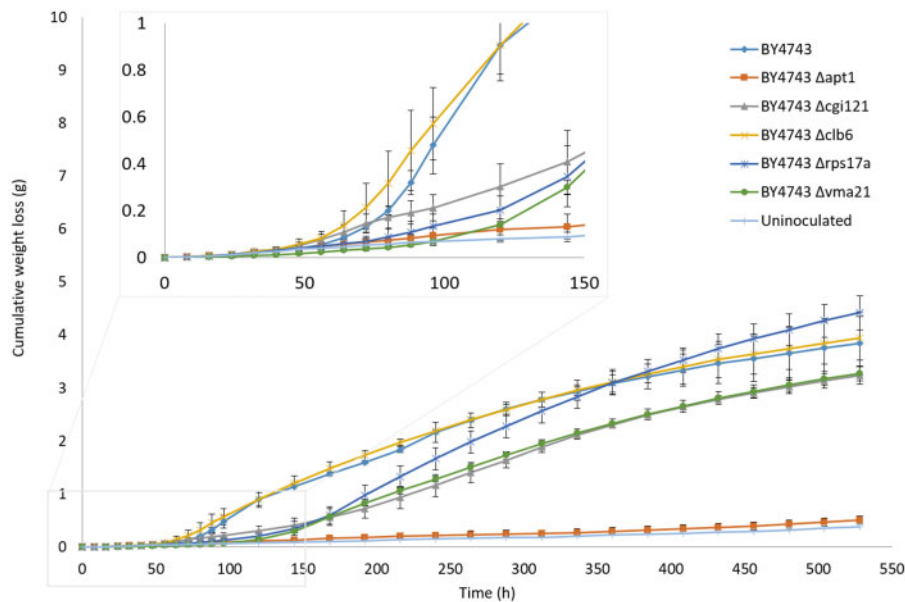
Figure 3 Average cumulative weight loss (g) of BY4743, BY4743 Δ*apt1*, BY4743 Δ*cgi121*, BY4743 Δ*clb6*, BY4743 Δ*rps17a*, and BY4743 Δ*vma21* fermented in SGM at 12.5°C for 528 h ($n = 3$). A blow-up of the graph is included to show the lag phase time more clearly. Error bars represent 95% confidence intervals.

the fermentation pre-cultures (Supplementary Figure S1), suggesting that this strain may either be deficient in a specific factor required for fermentation, the enological environment was not permissible for the growth of this strain, and/or a lack of nitrogen in the SGM limited nucleotide biosynthesis given that Apt1p is involved in the purine salvage pathway (Alfonzo *et al.* 1995). The lag phase duration was calculated for the remaining strains using a modified Gompertz curve-fitting model to obtain greater accuracy compared to the intercept method used in the quick screen (Tronchoni *et al.* 2009). Overall, lag times at 12.5°C compared to 15°C were approximately twofold longer, as expected when decreasing fermentation temperature (Charoenchai *et al.* 1998; Torija *et al.* 2003; Figure 4). The lag times confirm the prior observations from the weight loss curves in Figure 3, but with no significant difference between the lag times of the two fastest strains, BY4743 (64.9 h) and BY4743 Δ*clb1* (59.1 h) (Figure 4). The lag times of BY4743 Δ*cgi121* (149.6 h), BY4743 Δ*rps17a* (130.7 h), and BY4743 Δ*vma21* (119.9 h) were not significantly different from one another based on the 95% confidence intervals, but were significantly longer than the lag times of BY4743 and BY4743 Δ*clb6*.

To summarize, fermentation screening successfully identified three genes resulting in a longer lag phase when deleted (Δ*cgi121*, Δ*rps17a*, and Δ*vma21*). These were further investigated using single RHA.

Construction of RM11-1a and S288C single gene deletions and RHA hybrids reveals that the *CGI121* gene impacts on lag phase duration

To determine whether any of the three candidates, *CGI121* (Chr. XIII), *RPS17a* (Chr. XIII), or *VMA21* (Chr. VII), were responsible for the high LOD scores and genetic linkage to fermentative lag phase in the original 119 BY4716 × RM11-1a mapped progeny, single deletions of these three ORFs were constructed in two haploid *S. cerevisiae* strain backgrounds, RM11-1a (Hgm[R]) and S288C. S288C was used as a substitute for BY4716, as in Deed *et al.* (2017). For the three candidate genes, all combinations of RM11-1a and S288C single deletants with the corresponding wild-type

were hybridized for RHA (Table 2). Successful hybridization was confirmed using microsatellite typing (Table 4).

Fermentation in SGM at 12.5°C was performed for 192 h, with 8-hourly monitoring, using the RM11-1a and S288C parent strains, the haploid Δ*cgi121*, Δ*rps17a*, and Δ*vma21* single deletants in RM11-1a and S288C, the RM11-1a × S288C F_1 hybrid and the RHA F_1 hybrids constructed by crossing combinations of RM11-1a and S288C. The RHA hybrids were hemizygous for a null allele and either the RM11-1a copy or the S288C copy of *CGI121*, *RPS17a*, or *VMA21*. Cumulative weight loss curves show that the diploid RM11-1a × S288C F_1 hybrid had a superior fermentation performance compared to the haploid parents, RM11-1a and S288C, based on the emergence from fermentative lag and rate of fermentation (Figure 5, A–C). RM11-1a and S288C performed similarly, and in all cases exhibited a much shorter lag time compared to all RM11-1a and S288C single deletion mutants in Δ*cgi121*, Δ*rps17a*, and Δ*vma21*, in agreement with the results observed for BY4743. This result confirms that the presence of *CGI121*, *RPS17a*, and *VMA21* results in faster lag times. The RM11-1a × S288C Δ*cgi121* hybrid appeared to exit fermentative lag at the same time as RM11-1a × S288C, while the lag phase of RM11-1a Δ*cgi121* × S288C was longer (Figure 5A). There did not appear to be any difference between RM11-1a × S288C Δ*rps17a* or RM11-1a Δ*rps17a* × S288C in terms of fermentation performance, and potentially only a minor difference in lag time compared to RM11-1a × S288C (Figure 5B). The same trend was observed for RM11-1a × S288C Δ*vma21* and RM11-1a Δ*vma21* × S288C; however, both hemizygotes showed a noticeably longer lag time than RM11-1a × S288C (Figure 5C).

Figure 6A confirms that the lag times for RM11-1a and S288C Δ*cgi121*, Δ*rps17a*, and Δ*vma21* single deletants were significantly longer than nondeleted RM11-1a and S288C (average of 390 h compared to 126 h), as suggested from the weight loss curves in Figure 5, A–C. The long lag times of the deletion mutants corroborate the results shown by the BY4743 Δ*cgi121*, Δ*rps17a*, and Δ*vma21* deletants, but with even greater lag duration in RM11-1a and S288C due to the generally poor fermentation performance of haploid strains (Li *et al.* 2010). There were no significant
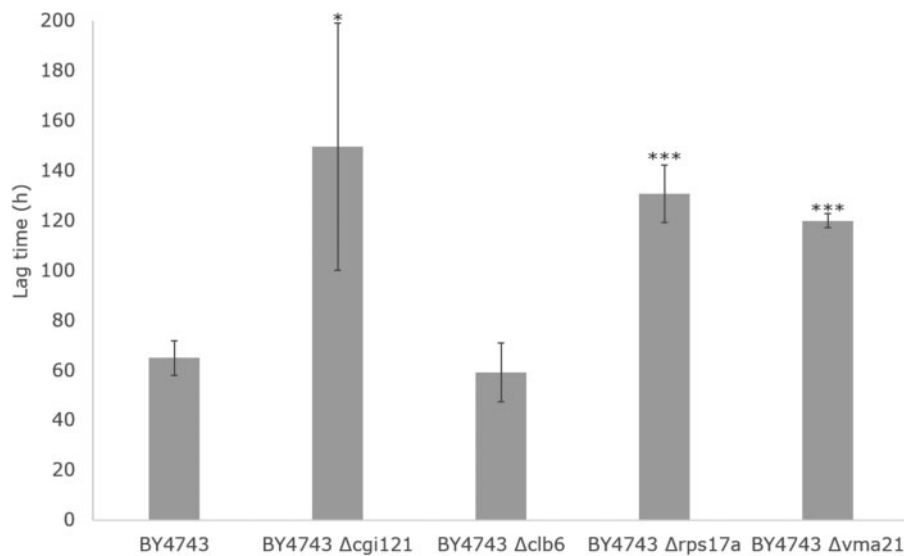
Figure 4 Lag time duration (h) of BY4743, BY4743 Δcgi121, BY4743 Δclb6, BY4743 Δrps17a, and BY4743 Δvma21 fermented in SGM at 12.5°C for 528 h ($n = 3$). Error bars represent 95% confidence intervals. Student's t-test was used to generate P-values between BY4743 and every single deletant (*$P < 0.05$, **$P < 0.01$, ***$P < 0.001$).

differences between the nondeleted RM11-1a and S288C strains or between the corresponding pairs of RM11-1a and S288c single deletion mutants in Δcgi121, Δrps17a, or Δvma21. In addition, there were no significant differences in lag time between RM11-1a Δcgi121, Δrps17a, and Δvma21 single deletants. The same result was observed for the S288C single deletants. For the RHA hybrids (Figure 6B), the lag time of the RM11-1a × S288C Δcgi121 hybrid was not significantly different from the RM11-1a × S288C wild type (average of 122 and 121 h, respectively). However, the RM11-1a Δcgi121 × S288C hybrid had a significantly longer lag time (149 h), suggesting that the presence of the RM11-1a CGI121 allele results in a lag time equivalent to wild type, but the S288C version results in increased lag time. This result is strong evidence validating the role of CGI121 on impacting the duration fermentative lag and corresponds to mapping data indicating that the longer lag time is consistent with the presence of the S288C CGI121 allele and not the RM11-1a copy in the homozygous F_1 progeny from the original cross (Deed et al. 2017). We aligned the RM11-1a and S288C nucleotide sequences of CGI121 to determine whether there were any allelic differences (Supplementary File S1). However, nucleotide alignment showed that the sequences were 99% identical and the single base difference observed at 282 bp (G in RM11-1a and A in S288C) was synonymous, with both codons corresponding to a phenylalanine (AAG vs. AAA). Further alignment of 1 kb in front of the coding sequence of the RM11-1a and S288C CGI121 sequences did not uncover any nucleotide differences in the promoter region. Because Cgi121p is one of five members of the endopeptidase-like and kinase associated to transcribed chromatin (EKC)/kinase, endopeptidase and other proteins of small size (KEOPS) protein complex (Srinivasan et al. 2011), we also aligned the RM11-1a and S288C nucleotide sequences for the four other genes, BUD32, GON7, KAE1, and PCC1 (Supplementary File S2). Nucleotide alignment for the RM11-1a and S288C BUD32 and PCC1 alleles were 100% identical, while the alignment for GON7 was 99.2% (3 bp) and was 99.7% for KAE3 (4 bp). All GON7 and KAE3 substitutions were synonymous.

For RPS17a, as suggested by the weight loss curves, there was no significant difference in lag time between RM11-1a × S288C Δrps17a or RM11-1a Δrps17a × S288C, suggesting that neither

allele impacts on lag time, even though RM11-1a Δrps17a × S288C did have a slightly longer lag than RM11-1a × S288C (138 h vs. 121 h). RM11-1a × S288C Δvma21 and RM11-1a Δvma21 × S288C were also not significantly different from one another, with no allele-specific impacts on lag duration for VMA21. The lag times for both hemizygotes were significantly longer than RM11-1a × S288C (144 and 149 h vs. 121 h) suggesting an additive effect with two copies of the VMA21 gene being beneficial for a shorter lag time.

Overall, these results have demonstrated a clear role of CGI121 on Chr. XIII for altering fermentative lag time, and although RPS17a and VMA21 did not show allelic differences in terms of their impact on lag time, both genes have a clear effect on lag duration when deleted.

Discussion

Through genetic linkage analysis from a set of completely mapped 119 BY4716 × RM11-1a F_1 progeny, fermentation screening of single BY4743 deletants in candidate genes to narrow down the field, and RHA using RM11-1a and S288C, we have identified the relationship between the CGI121 gene on Chr. XIII with fermentative lag time duration, which likely corresponds to the high LOD score on Chr. XIII (Deed et al. 2017). Deletion of Δcgi121 in homozygous diploid BY4743, and haploids RM11-1a and S288C, resulted in a significant increase in fermentative lag in SGM at 12.5°C, compared to the corresponding wild types. The effect of the CGI121 gene in fermentative lag phase was different in the hemizygous single RHA F_1 hybrids, depending on whether they harbored the RM11-1a or the S288C allele, i.e., the RM11-1a Δcgi121 × S288C F_1 hybrid had a significantly longer fermentative lag duration than RM11-1a × S288C and RM11-1a × S288C Δcgi121. Mapping data from Deed et al. (2017) determined that the difference in CGI121 in the F_1 progeny was derived from the S288C allele. Transcriptomics data also demonstrated that CGI121 transcripts are upregulated by at least twofold in an M2 × S288C F_1 hybrid versus the M2 parent during the early stages of fermentation (at 2% weight loss) at 12.5°C, suggesting a key difference in the regulation of the S288C CGI121 allele.
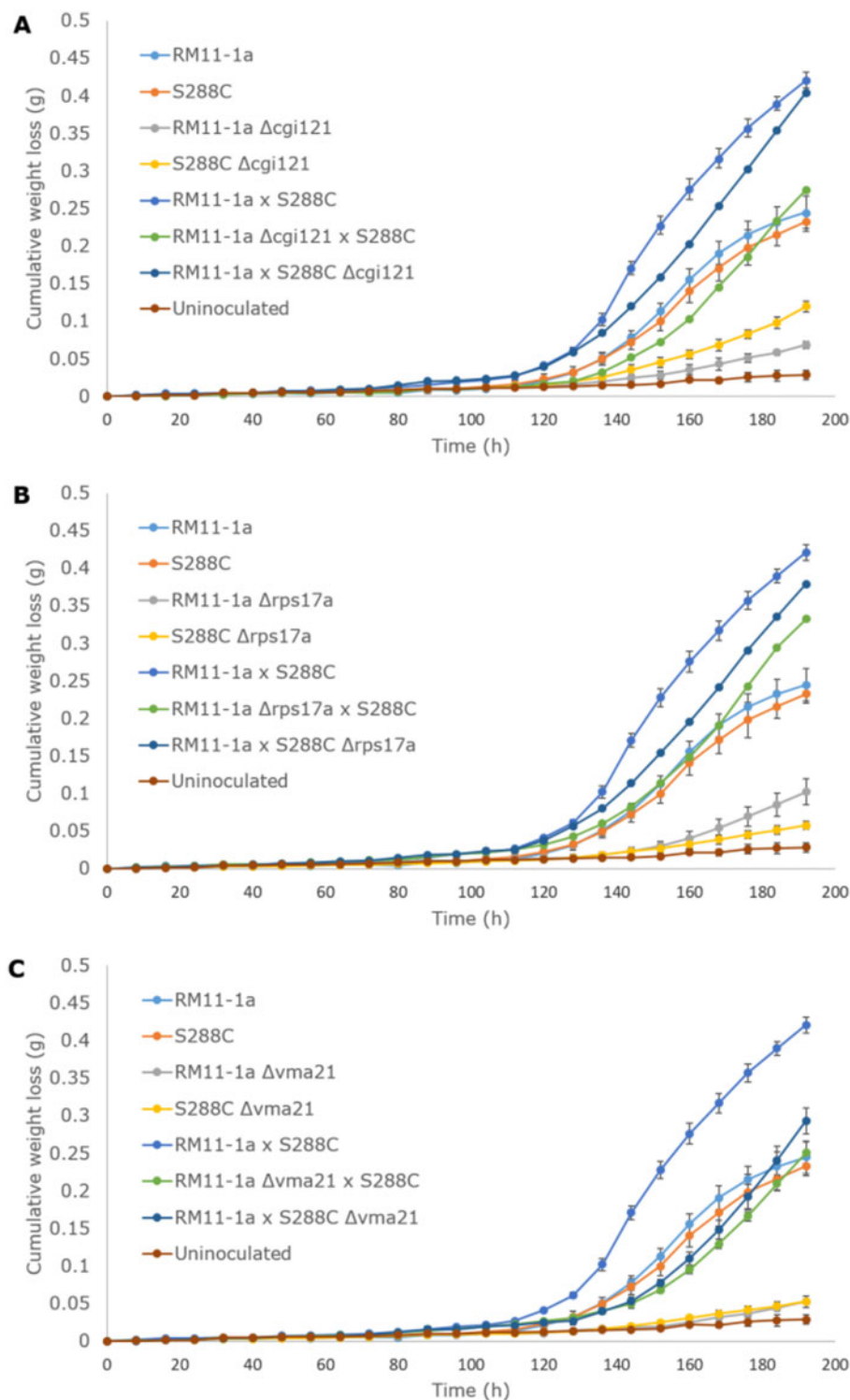
Figure 5 Average cumulative weight loss (g) of RM11-1a, S288C, and their corresponding single deletants and RHA hybrids for *CGI121* (A), *RPS17a* (B), and *VMA21* (C) fermented in SGM at 12.5°C for 192 h ($n = 3$). Error bars represent 95% confidence intervals.

Although the single nucleotide difference between the RM11-1a and S288C *CGI121* alleles was synonymous, it has been reported that synonymous mutations can result in differences in gene expression, with the use of particular codons significantly increasing transcript numbers (Plotkin and Kudla 2011). In addition, *CGI121* contains an intron at 457–562 bp, which is a relatively uncommon feature of yeast protein-coding genes (only

5%). Differences in the regulation of genes from strain to strain can be caused by variation in intron splicing efficiencies, which can be modulated by the stress response (Pleiss *et al.* 2007). The *CGI121* intron is also classified as having an unstable and unstructured branch point (BP) (Gahura *et al.* 2011) and a predicted novel type of BP (Gould *et al.* 2016), which may further impact on splicing efficiency. Therefore, it would be interesting to
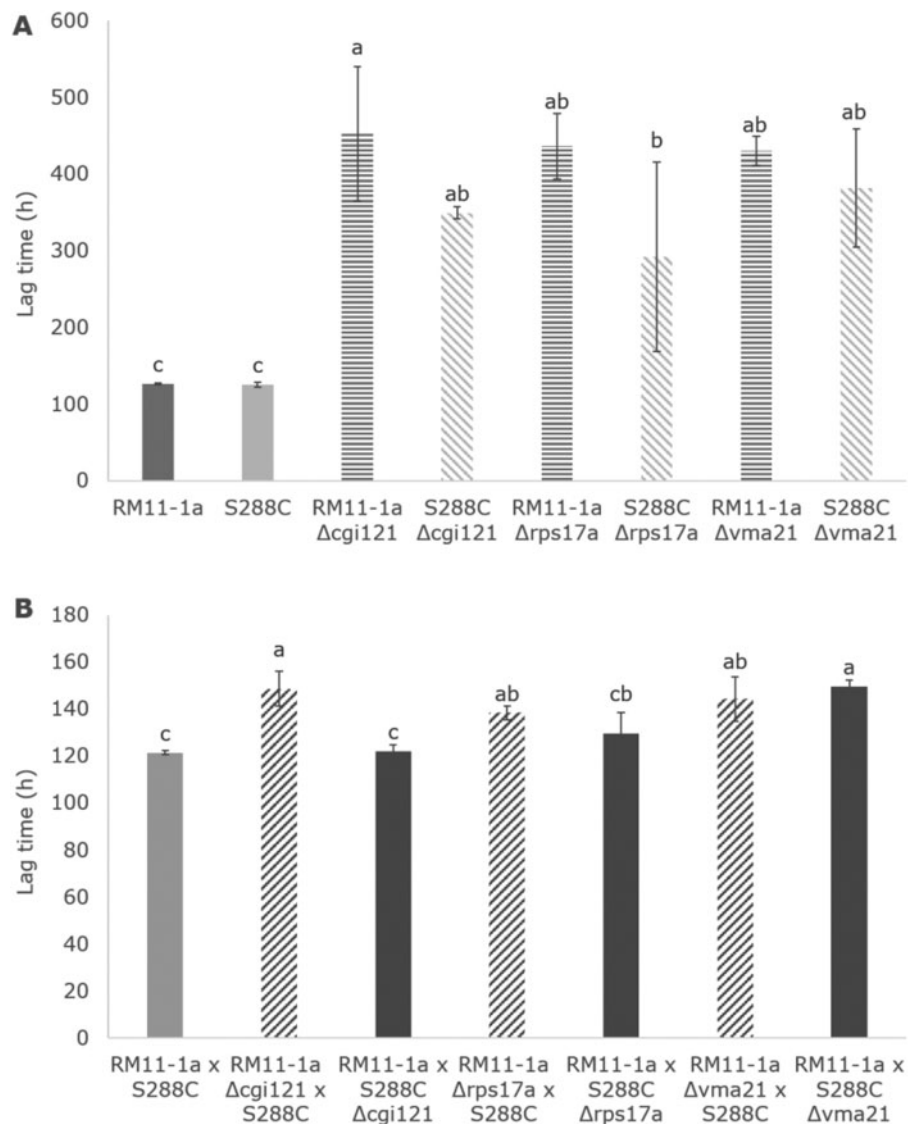
Figure 6 Lag time duration (h) of RM11-1a, S288C, and respective single deletants in Δ*cgi121*, Δ*rps17a*, and Δ*vma21* (A) and RHA hybrids comparing the impact of RM11-1a and S288C alleles of *CGI121*, *RPS17a*, and *VMA21* (B) fermented in SGM at 12.5°C for 192 h ($n = 3$). Error bars represent 95% confidence intervals. Samples sharing the same letter are not significantly different (ANOVA followed by *post-hoc* Tukey's HSD).

determine whether the splicing efficiencies of the RM11-1a and S288C *CGI121* introns are different. Alternatively, there could be *cis* or *trans* regulatory effects depending on the *CGI121* allele position (Brem *et al.* 2002; Sinha *et al.* 2006). Investigation into whether any of the other members of the EKC/KEOPS complex displayed allelic difference in RM11-1a compared to S288C did not provide any important differences, with only synonymous base changes, highlighting how highly conserved this complex is (Srinivasan *et al.* 2011).

Role of *CGI121* and evidence for impact on fermentative lag time

CGI121 (*YML036W*) is a 652 bp gene encoding a small polypeptide component EKC/KEOPS protein complex with roles in transcription, telomere uncapping, chromosome segregation, and DNA repair, and is specifically required for threonine carbamoyl adenosine (t^6A) tRNA modification and telomeric TG_{1-3} recombination and length regulation (Kisseleva-Romanova *et al.* 2006; Srinivasan *et al.* 2011; Liu *et al.* 2018). There are five proteins within this complex, encoded by *BUD32*, *CGI121*, *GON7*,

KAE1, and *PCC1*. Of the five genes, only Δ*kae1* null mutants are inviable, due to the severe growth impairment and chromosomal instability caused by deleting this essential gene, which encodes an ATPase (Downey *et al.* 2006; Mao *et al.* 2008). The role of Cgi121p in the EKC/KEOPS complex is to regulate Bud32p kinase activity by interacting with the N-terminal lobe, which in turn regulates the Kae1p ATPase, allowing for downstream function and catalytic activities (Mao *et al.* 2008; Zhang *et al.* 2015). Cgi121p does not directly participate in the t^6A tRNA modification function of the complex, but is important for telomere length regulation and recombination (Downey *et al.* 2006; Srinivasan *et al.* 2011; Peng *et al.* 2015), and may also be involved in creating stable connections between each KEOPS subunit, allowing for correct assembly (Perrochia *et al.* 2013). In the *S. cerevisiae* EKC/KEOPS complex, Cgi121p is not required for retaining functionality but is required for maximal activity, with the phenotypes of Δ*cgi121* mutants being much milder than those displayed by Δ*bud32*, Δ*kae1* or Δ*pcc1* mutants (Downey *et al.* 2006; Kisseleva-Romanova *et al.* 2006; Mao *et al.* 2008; Perrochia *et al.* 2013).

Classical genetics studies have shown that null mutants of Δ*cgi121* have increased replicative lifespan and viability, and reduced single-stranded DNA at uncapped telomeres which functions to initiate telomere recombination (Downey *et al.* 2006; Peng *et al.* 2015). Deletion of Δ*cgi121* in BY4742 resulted in cells with a 50% longer lifespan, as the absence of *CGI121* inhibits telomere recombination and therefore provides greater genome stability (Peng *et al.* 2015). Large-scale surveys have implicated the Δ*cgi121* deletion in causing reduced vegetative and fermentative growth rates; however, data from Srinivasan *et al.* (2011) suggests that the vegetative growth of a W303-1A Δ*cgi121* mutant was close to wild type on solid medium after two days growth at 30°C. In the propagation of BY4743 Δ*cgi121* for fermentation in this research there did not appear to be any difference in vegetative growth in YPD compared to BY4743, with equivalent cell titres (data not shown), but there could be a difference in lag phase earlier on in vegetative growth which was not observable after 24 h of growth at 28°C. In terms of fermentative growth, Δ*cgi121* was identified by Steinmetz *et al.* (2002a) as showing reduced growth on YPD with 2% glucose; however, this screen was aerobic and does not adequately represent the fermentation environment. Hoose *et al.* (2012) identified S288C mutants in Δ*cgi121* as having an increased duration of cell cycle progression in G_1 phase, with the percentage of S288C Δ*cgi121* G_1 cells greater than two standard deviations (41.6%) above wild-type S288C at equivalent measurement times. The longer period spent in G_1 phase would mean that Δ*cgi121* cells do not divide as often as wild type and can explain the longer lag time during fermentation. Cell division and vegetative growth influences the timeframe of the fermentative lag phase and stressful environmental conditions, such as those encountered in the enological environment can significantly prolong G_1 (Hoose *et al.* 2012), which could be why the impact of the Δ*cgi121* was more pronounced during fermentation at low temperature. The presence of certain nutrients also influences the timing through G_1 to START, from where the rest of the growth cycle can be completed. When shifting from poor to rich medium, the G_1 phase can be prolonged temporarily until the cells reach a critical size allowing them to commit to a phase of cell division (Hoose *et al.* 2012). In Δ*cgi121* mutants, there is a decreased rate of carbon and nitrogen utilization, with abnormal glucose and arginine metabolism (VanderSluis *et al.* 2014), as well as an upregulation of carbohydrate metabolism genes in Δ*cgi121* mutants compared to wild type (Chou *et al.* 2017). Therefore, abnormal usage of glucose, a primary carbon source in grape juice and SGM, as well as decreased nitrogen consumption and accumulation of arginine, could greatly influence the lag duration of Δ*cgi121* mutants during fermentation.

Impact of *RPS17a* and *VMA21* on fermentative lag duration

We have also shown that along with the single deletion in Δ*cgi121*, single deletions in Δ*rps17a* [encoding a ribosomal protein of the small 40S subunit (Abovich *et al.* 1985)], and Δ*vma21* [encoding an integral membrane protein required for V-ATPase function (Hill and Stevens 1994)] resulted in an extended lag time duration in BY4743, RM11-1a, and S288C; however, neither *RPS17a* nor *VMA21* provided clear evidence for any allelic differences via RHA analysis. Interestingly, Δ*rps17a* mutants demonstrate a prolonged G_1 phase in the cell cycle, in the same way as Δ*cgi121* (Hoose *et al.* 2012), which could explain the influence of the null mutant on fermentative lag. Null mutations in Δ*vma21*, result in a multitude of phenotypes in *S. cerevisiae*, with decreased resistance to oxidative and osmotic stress (Dudley *et al.* 2005), and decreased thermotolerance (Jarolim *et al.* 2013), all of which can result in a longer fermentative lag time (Ferreira *et al.* 2017). Although Δ*vma21* mutants also had a decreased carbon utilization rate, these were for nonfermentable carbon sources (Dudley *et al.* 2005; VanderSluis *et al.* 2014). The QTL responsible for the high LOD score on Chr. VII in Deed *et al.* (2017) is yet to be identified, but may be derived from the RM11-1a parent, which would mean that the initial BY4743 screen was not so useful for pinpointing the QTL responsible. Future work could investigate whether any of the seven essential genes that were not assessed out of the original 44 candidates play a role in lag duration, by screening for evidence of haploinsufficiency in the fermentative lag phenotypes of diploids that are hemizygous at these loci.

Conclusions

We have shown that single deletions of Δ*cgi121*, Δ*rps17a*, and Δ*vma21* result in increased fermentative lag duration in *S. cerevisiae*. This research has also demonstrated that the *CGI121* gene, encoding a component of the EKC/KEOPS complex, plays a role in modulating the fermentative lag phase in *S. cerevisiae*. RHA confirmed that the S288C-derived *CGI121* allele accounted for a longer lag time. A greater understanding of the role of the *CGI121* in stress tolerance will allow easier manipulation and/or selection of *S. cerevisiae* strains to shorten or lengthen lag time and provide growth advantages during the fermentation of foods and beverages.

Literature cited

Abovich N, Gritz L, Tung L, Rosbash M. 1985. Effect of *RP51* gene dosage alterations on ribosome synthesis in *Saccharomyces cerevisiae*. Mol Cell Biol 5:3429–3435.

Albertin W, Zimmer A, Miot-Sertier C, Bernard M, Coulon J, *et al.* 2017. Combined effect of the *Saccharomyces cerevisiae* lag phase and the non-*Saccharomyces* consortium to enhance wine fruitiness and complexity. Appl Microbiol Biotechnol 101:7603–7620.

Alfonzo JD, Sahota A, Deeley MC, Ranjekar P, Taylor MW. 1995. Cloning and characterization of the adenine phosphoribosyltransferase-encoding gene (*APT1*) from *Saccharomyces cerevisiae*. Gene 161:81–85.

Baty F, Ritz C, Charles S, Brutsche M, Flandrois J-P, *et al.* 2015. A toolbox for nonlinear regression in R: The package nlstools. J Stat Soft 66:1–21.

Beltran G, Rozès N, Mas A, Guillamón JM. 2007. Effect of low-temperature fermentation on yeast nitrogen metabolism. World J Microbiol Biotechnol 23:809–815.

Bely M, Sablayrolles JM, Barre P. 1990. Description of alcoholic fermentation kinetics: its variability and significance. Am J Enol Viticulture 41:319–324.

Bisson LF. 1999. Stuck and sluggish fermentations. Am J Enol Viticulture 50:107–119.

Brem RB, Yvert G, Clinton R, Kruglyak L. 2002. Genetic dissection of transcriptional regulation in budding yeast. Science 296:752–755.

Camarasa C, Sanchez I, Brial P, Bigey F, Dequin S. 2011. Phenotypic landscape of *Saccharomyces cerevisiae* during wine fermentation: evidence for origin-dependent metabolic traits. PLoS One 6: e25147.

Charoenchai C, Fleet GH, Henschke PA. 1998. Effects of temperature, pH, and sugar concentration on the growth rates and cell biomass of wine yeasts. Am J Enol Viticulture 49:283–288.

Chou HJ, Donnard E, Gustafsson HT, Garber M, Rando OJ. 2017. Transcriptome-wide analysis of roles for tRNA modifications in translational regulation. Mol Cell 68:978–992.e974.

Colombie S, Malherbe S, Sablayrolles JM. 2005. Modeling alcoholic fermentation in enological conditions: feasibility and interest. Am J Enol Viticulture 56:238–245.

Deed RC, Fedrizzi B, Gardner RC. 2017. *Saccharomyces cerevisiae FLO1* gene demonstrates genetic linkage to increased fermentation rate at low temperatures. G3 (Bethesda). 7:1039–1048.

Deed RC, Hou R, Kinzurik MI, Gardner RC, Fedrizzi B. 2019. The role of yeast *ARO8*, *ARO9* and *ARO10* genes in the biosynthesis of 3-(methylthio)-1-propanol from L-methionine during fermentation in synthetic grape medium. FEMS Yeast Res. 19:1–9.

Downey M, Houlsworth R, Maringele L, Rollie A, Brehme M, *et al.* 2006. A genome-wide screen identifies the evolutionarily conserved KEOPS complex as a telomere regulator. Cell 124: 1155–1168.

Dudley AM, Janse DM, Tanay A, Shamir R, Church GM. 2005. A global view of pleiotropy and phenotypically derived gene function in yeast. Mol Syst Biol. 1:

Ferreira D, Galeote V, Sanchez I, Legras JL, Ortiz-Julien A, *et al.* 2017. Yeast multistress resistance and lag-phase characterisation during wine fermentation. FEMS Yeast Res. 17:1–11.

Gahura O, Hammann C, Valentová A, Půta F, Folk P. 2011. Secondary structure is required for 3′ splice site recognition in yeast. Nucleic Acids Res. 39:9759–9767.

Ganucci D, Guerrini S, Mangani S, Vincenzini M, Granchi L. 2018. Quantifying the effects of ethanol and temperature on the fitness advantage of predominant *Saccharomyces cerevisiae* strains occurring in spontaneous wine fermentations. Front Microbiol. 9:1563.

García-Ríos E, Morard M, Parts L, Liti G, Guillamón JM. 2017. The genetic architecture of low-temperature adaptation in the wine yeast *Saccharomyces cerevisiae*. BMC Genomics 18:159.

García-Ríos E, Ramos-Alonso L, Guillamón JM. 2016. Correlation between low temperature adaptation and oxidative stress in *Saccharomyces cerevisiae*. Front Microbiol. 7:1199.

Gould GM, Paggi JM, Guo Y, Phizicky DV, Zinshteyn B, *et al.* 2016. Identification of new branch points and unconventional introns in *Saccharomyces cerevisiae*. RNA. 22:1522–1534.

Harsch MJ, Lee SA, Goddard MR, Gardner RC. 2010. Optimized fermentation of grape juice by laboratory strains of *Saccharomyces cerevisiae*. FEMS Yeast Res. 10:72–82.

Henschke PA, Jiranek V. 1993. Yeasts - Metabolism of Nitrogen Compounds. Newark, NJ: Harwood Academic Publishers.

Hill KJ, Stevens TH. 1994. Vma21p is a yeast membrane protein retained in the endoplasmic reticulum by a di-lysine motif and is required for the assembly of the vacuolar H+-ATPase complex. Mol Biol Cell 5:1039–1050.

Hoose SA, Rawlings JA, Kelly MM, Leitch C, Ababneh QO, *et al.* 2012. A systematic analysis of cell cycle regulators in yeast reveals that most factors act independently of cell size to control initiation of division. PLoS Genet. 8:e1002590.

Jarolim S, Ayer A, Pillay B, Gee AC, Phrakaysone A, *et al.* 2013. *Saccharomyces cerevisiae* genes involved in survival of heat shock. G3 (Bethesda). 3:2321–2333.

Kinzurik MI, Herbst-Johnstone M, Gardner RC, Fedrizzi B. 2015. Evolution of volatile sulfur compounds during wine fermentation. J Agric Food Chem. 63:8017–8024.

Kisseleva-Romanova E, Lopreiato R, Baudin-Baillieu A, Rousselle JC, Ilan L, *et al.* 2006. Yeast homolog of a cancer-testis antigen defines a new transcription complex. EMBO J. 25:3576–3585.

Li BZ, Cheng JS, Ding MZ, Yuan YJ. 2010. Transcriptome analysis of differential responses of diploid and haploid yeast to ethanol stress. J Biotechnol. 148:194–203.

Liu YY, He MH, Liu JC, Lu YS, Peng J, *et al.* 2018. Yeast KEOPS complex regulates telomere length independently of its t6A modification function. J Genet Genomics 45:247–257.

Llauradó JM, Rozès N, Bobet R, Mas A, Constantí M. 2002. Low temperature alcoholic fermentations in high sugar concentration grape musts. J Food Sci. 67:268–273.

Llauradó JM, Rozès N, Constanti M, Mas A. 2005. Study of some *Saccharomyces cerevisiae* strains for winemaking after preadaptation at low temperatures. J Agric Food Chem. 53:1003–1011.

López-Malo M, Querol A, Guillamon JM. 2013. Metabolomic comparison of *Saccharomyces cerevisiae* and the cryotolerant species *S. bayanus* var. *uvarum* and *S. kudriavzevii* during wine fermentation at low temperature. PLoS One 8:e60135.

Mao DYL, Neculai D, Downey M, Orlicky S, Haffani YZ, *et al.* 2008. Atomic structure of the KEOPS complex: an ancient protein kinase-containing molecular machine. Mol Cell 32:259–275.

Marullo P, Aigle M, Bely M, Masneuf-Pomarède I, Durrens P, *et al.* 2007. Single QTL mapping and nucleotide-level resolution of a physiologic trait in wine *Saccharomyces cerevisiae* strains. FEMS Yeast Res. 7:941–952.

Marullo P, Bely M, Masneuf-Pomarède I, Pons M, Aigle M, *et al.* 2006. Breeding strategies for combining fermentative qualities and reducing off-flavor production in a wine yeast model. FEMS Yeast Res. 6:268–279.

Molina AM, Swiegers JH, Varela C, Pretorius IS, Agosin E. 2007. Influence of wine fermentation temperature on the synthesis of yeast-derived volatile aroma compounds. Appl Microbiol Biotechnol. 77:675–687.

Peltier E, Sharma V, Martí Raga M, Roncoroni M, Bernard M, *et al.* 2018. Dissection of the molecular bases of genotype x environment interactions: a study of phenotypic plasticity of *Saccharomyces cerevisiae* in grape juices. BMC Genomics 19:772.

Peng J, He MH, Duan YM, Liu YT, Zhou JQ. 2015. Inhibition of Telomere Recombination by Inactivation of KEOPS Subunit Cgi121 Promotes Cell Longevity. PLoS Genet. 11:e1005071.

Perez-Ortin JE, Querol A, Puig S, Barrio E. 2002. Molecular characterization of a chromosomal rearrangement involved in the adaptive evolution of yeast strains. Genome Res. 12:1533–1539.

Perrochia L, Guetta D, Hecker A, Forterre P, Basta T. 2013. Functional assignment of KEOPS/EKC complex subunits in the biosynthesis of the universal t6A tRNA modification. Nucleic Acids Res. 41: 9484–9499.

Pleiss JA, Whitworth GB, Bergkessel M, Guthrie C. 2007. Rapid, transcript-specific changes in splicing in response to environmental stress. Mol Cell 27:928–937.

Plotkin JB, Kudla G. 2011. Synonymous but not the same: The causes and consequences of codon bias. Nat Rev Genet. 12:32–42.

Redón M, Guillamón JM, Mas A, Rozès N. 2011. Effect of growth temperature on yeast lipid composition and alcoholic fermentation at low temperature. Eur Food Res Technol. 232:517–527.

Richards KD, Goddard MR, Gardner RC. 2009. A database of microsatellite genotypes for *Saccharomyces cerevisiae*. Antonie Van Leeuwenhoek 96:355–359.

Rossignol T, Dulau L, Julien A, Blondin B. 2003. Genome-wide monitoring of wine yeast gene expression during alcoholic fermentation. Yeast 20:1369–1385.

Salvadó Z, Chiva R, Rodriguez-Vargas S, Randez-Gil F, Mas A, *et al.* 2008. Proteomic evolution of a wine yeast during the first hours of fermentation. FEMS Yeast Res. 8:1137–1146.

Schiestl RH, Gietz RD. 1989. High efficiency transformation of intact yeast cells using single stranded nucleic acids as a carrier. Curr Genet 16:339–346.

Sinha H, Nicholson BP, Steinmetz LM, McCusker JH. 2006. Complex genetic interactions in a quantitative trait locus. PLoS Genet. 2: e13.

Srinivasan M, Mehta P, Yu Y, Prugar E, Koonin EV, *et al.* 2011. The highly conserved KEOPS/EKC complex is essential for a universal tRNA modification, t6A. EMBO J. 30:873–881.

Steinmetz LM, Scharfe C, Deutschbauer AM, Mokranjac D, Herman ZS, *et al.* 2002a. Systematic screen for human disease genes in yeast. Nat Genet. 31:400–404.

Steinmetz LM, Sinha H, Richards DR, Spiegelman JI, Oefner PJ, *et al.* 2002b. Dissecting the architecture of a quantitative trait locus in yeast. Nature 416:326–330.

Torija MJ, Rozes N, Poblet M, Guillamon JM, Mas A. 2003. Effects of fermentation temperature on the strain population of *Saccharomyces cerevisiae*. Int J Food Microbiol. 80:47–53.

Treu L, Campanaro S, Nadai C, Toniolo C, Nardi T, *et al.* 2014. Oxidative stress response and nitrogen utilization are strongly variable in *Saccharomyces cerevisiae* wine strains with different fermentation performances. Appl Microbiol Biotechnol. 98: 4119–4135.

Tronchoni J, Gamero A, Arroyo-López FN, Barrio E, Querol A. 2009. Differences in the glucose and fructose consumption profiles in diverse *Saccharomyces* wine species and their hybrids during grape juice fermentation. Int J Food Microbiol. 134:237–243.

VanderSluis B, Hess DC, Pesyna C, Krumholz EW, Syed T, *et al.* 2014. Broad metabolic sensitivity profiling of a prototrophic yeast deletion collection. Genome Biol. 15:R64.

Zhang W, Collinet B, Graille M, Daugeron MC, Lazar N, *et al.* 2015. Crystal structures of the Gon7/Pcc1 and Bud32/Cgi121 complexes provide a model for the complete yeast KEOPS complex. Nucleic Acids Res. 43:3358–3372.

Communicating editor: B. Andrews